Effect of the spin crossover filler concentration on the performance of composite bilayer actuators

Mario Piedrahita-Bello, Yue Zan, Alejandro Enriquez-Cabrera, Gábor Molnár, Bertrand Tondu, L. Salmon, Azzedine Bousseksou

Effect of the spin crossover filler concentration on the performance of composite bilayer actuators

Mario Piedrahita-Bello,[1,2] Yue Zan,[1] Alejandro Enriquez-Cabrera[1], Gábor Molnár,[1] Bertrand Tondu,[2] Lionel Salmon,[1,*] Azzedine Bousseksou[1,*]

[1]LCC, CNRS & Université de Toulouse (UPS, INP), 31077 Toulouse, France

[2]LAAS, CNRS & Université de Toulouse (UPS, INSA), 31400 Toulouse, France

Lionel.salmon@lcc-toulouse.fr, azzedine.bousseksou@lcc-toulouse.fr

Abstract. Macroscopic, soft bilayer spin crossover@polymer actuators were fabricated by a blade casting technique using $[Fe(NH_2trz)_3]SO_4$ spin crossover particles embedded in a P(VDF-TrFE) matrix. Incorporation of silver flakes in the second layer allowed for electro-thermal actuation via Joule heating. The speed and amplitude of the actuator bending movement, resulting from the expansion/contraction of the spin crossover particles on heating/cooling, were tested for different particle concentrations (15, 25, 33 and 50 wt%) under both open- and closed-loop controls. The capability of the actuators to embark charge and to follow a sinusoidal position was also investigated.

1. Introduction

In the past few years, there have been an increasing interest in the use of ferrous spin crossover (SCO) complexes for mechanical transduction [1–3], exploiting the large, reversible volume expansion (up to 10 – 15 %) [4–7] that accompanies the spin transition phenomenon when going from the low spin (LS) to the high spin (HS) state of the central metal ion [8–9]. This property allows SCO materials to transduce into mechanical work the various stimuli (thermal, optical, chemical …) that can trigger the SCO phenomenon. Previous work in this line of research has seen significant progress, going from an initial proof of concept [3] to electrothermally driven actuators [10], sensors [11-13], generators [14-15], microactuators [16–20] and 3D-printed macroscopic actuators [21].

In this context, we have recently synthesized high quality, homogeneous SCO@P(VDF-TrFE) composites (P(VDF-TrFE) = poly(vinylidene fluoride-trifluoro-ethylene) using a blade casting technique. When combined with a second layer of Ag@P(VDF-TrFE) a bending bilayer actuator was obtained, which can be actuated by Joule effect [22]. By implementing a closed-loop control, these devices turned out to be very efficient, in terms of work output (>4 J/cm^3), controllability (>99% accuracy), life cycle (> 36000) and versatility, via different particle compositions and morphologies. These results provide a tangible scope for the use of SCO particle based polymer composites for applications in soft robotics and related fields.

In the present work, we discuss novel results towards the optimization of the work output of these bilayer actuators. Notably, we have investigated the relationship between the concentration of the SCO filler in a composite actuator and the actuation properties, including deflection amplitude, speed and controllability. To this aim we fabricated a series of bilayer actuators based on the $[Fe(NH_2trz)_3]SO_4$ SCO complex (NH_2trz = 1,2,4-4-NH_2-triazole) [21, 23-24], modifying the proportion of SCO material in the active layer with respect to the initially used 25% SCO filler [22]. Compounds from this family forming 1-D polymeric chains are often studied because they present versatile properties in terms of transition temperature with the possibility to be nanostructured while maintaining interesting spin crossover properties [25-27].

The study of the filler concentration is obviously a key parameter because it allows to modulate not only the actuating properties, but also, in certain cases, the thermomechanical and/or the electrical properties of the active layer. For example, it was shown that the increase of quartz concentration in a dielectric elastomer can enhance the dielectric properties, resulting in an increased actuation amplitude [28]. Similar improvement was obtained while increasing the magnetic filler concentration in magnetic polymer composites, resulting also in the increase of the material stiffness [29]. For certain composite materials, however, the improvement of the actuation properties by the increase of the active filler can be detrimental to the mechanical (strength, stiffness,..) and/or electrical (percolation limit, charge accumulation,..) properties of the device and an optimal filler concentration have to be established to achieve a compromise. This effect can be illustrated for instance by the spontaneous decrease of the magnitude of the actuation stroke beyond 2 wt % loading of carbon nanotubes in polymer-nanotube composites [30].

2. Materials and methods

All solvents and reagents were purchased from Sigma Aldrich and used without further purification. The synthesis and characterization of the spin crossover complex $[Fe(NH_2trz)_3]SO_4$ has been previously reported [21]. For the fabrication and characterization of the bilayer actuator devices, we followed the same methodology as described in ref. [22]. The SCO@P(VDF-TrFE) composite films were prepared by dispersing the SCO complex $[Fe(NH_2trz)_3]SO_4$ (45, 90, 120 and 180 mg for 15, 25, 33 and 50 wt % composites, respectively) in 2-butanone (1.8 mL) in an ultrasonic bath for 40 min. Then, the P(VDF-TrFE) 70/30 copolymer (270, 270, 240 and 180 mg for 15, 25, 33 and 50 wt % composites, respectively) was added to the mixture and dissolved at 45 °C. The resulting suspensions were then blade-cast at a height of 1.5 mm on a heated Teflon surface at 50 °C and kept at this temperature for 10 minutes, until the composite was dry. On top of this first layer, an electrically conductive layer was then prepared. For this, we dispersed 10 µm Ag flakes (318 mg) in 2-butanone (1.8 mL) in an ultrasonic bath for 5 min. Then, the P(VDF-TrFE) copolymer (216 mg) was added to the mixture and dissolved at 45 °C. The resulting suspensions were then blade-cast at a height of 1.5 mm on top of the dry SCO@P(VDF-TrFE) layer at 50 °C and kept at this temperature for ca. 2 h, until the composite was completely dry. The bilayer films were then annealed at 105 °C for 12 h. Bilayer devices with size 30 x 20 x 0.15 mm^3 were then cut into a U-shape (Fig. 1a) using a Realmeca RV 2-SP high precision lathe by attaching the bilayer films to an aluminum support.

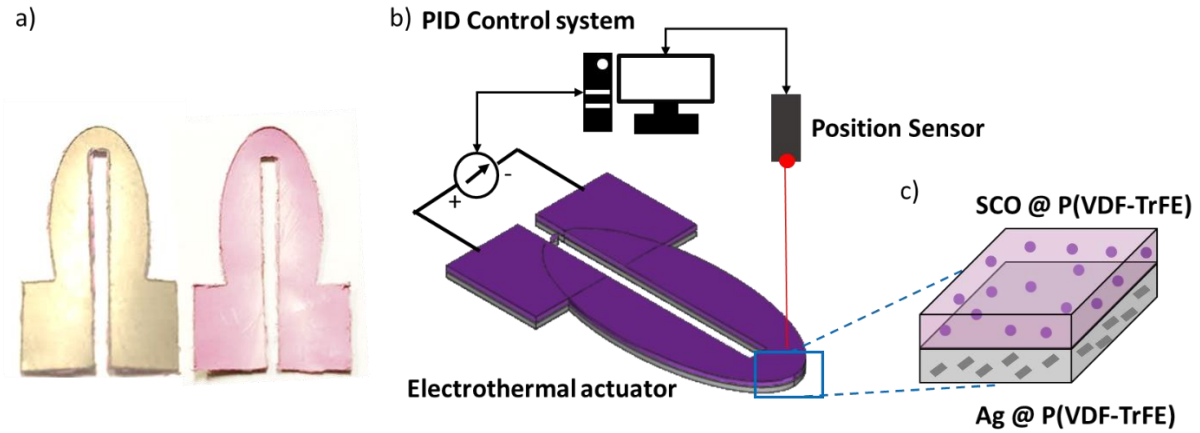

Fig. 1. Bilayer actuator devices. a) Photograph of an actuator device showing the grey conductive layer (left) and the pink SCO layer (right). b) Scheme of the actuator test bench indicating the Joule heating, the optical displacement detection and the PID control. c) Actuators composition.

Scanning electron microscopy (SEM) images were acquired using a JEOL JSM 7800F Prime instrument operated at 5 kV. Samples for SEM were prepared by breaking the film cooled by liquid nitrogen and the cross-section was metalized with Pt. Variable temperature (0.5 °C/min) optical reflectivity measurements on all bilayers were conducted simultaneously with the analysis of the bulk SCO powder using a stereomicroscope (SMZ-168, Motic) equipped with a color camera (MOTICam 1000) and a heating-cooling stage (Linkam THMS-600). For the actuator control experiments, a Keithley 2420 source-meter unit was used to provide the input current for electro-thermal actuation. Position tracking of the tip bending of the actuator devices was performed using a Micro-Epsilon opto-NCDT 2300 laser triangulation system (Fig. 1b). The LabVIEW software was used both for open- and closed-loop control. The latter was achieved by means of conventional PID control [22]. The temperature of the samples was mapped via a Micro Epsilon 640 Thermal Imager.

3. Results and discussion

In agreement with previous reports [21], the obtained $[Fe(NH_2trz)_3]SO_4$ complex presents a thermal spin transition at 73 °C and 61 °C on heating and cooling, respectively, as shown by the thermal variation of its optical reflectivity (Fig. 2a). We charged the P(VDF-TrFE) matrix by the microcrystalline powder of $[Fe(NH_2trz)_3]SO_4$ at four different concentrations of the SCO material: 15 (**1**), 25 (**2**), 33 (**3**) and 50 (**4**) wt%. As shown in Figure 2a, for each composite sample, the thermal variation of the optical reflectivity indicates similar spin crossover properties, albeit at somewhat lower temperatures (ca. 70 and 56 °C) when compared to the bulk powder. Such differences are not unusual in SCO@polymer composites [31] and are usually ascribed to particle-matrix interactions and/or to different heat transfer in the composite (vs. the powder). On the other hand, the particle concentration has no substantial impact on the SCO curves in the investigated range. SEM images acquired on the bilayer cross-sections are shown in Figures 2b-2e and Figure S1 in the Electronic Supporting Information (ESI). The separation of the two layers is neat, yet the common polymer backbone allows to maintain the mechanical integrity of the bilayer over numerous actuation cycles. Indeed, we have never encountered delamination, which is usually the major flaw of this type of bending bilayer devices. One can clearly distinguish also the rod-shaped SCO particles (ca. 1 micron

mean length), which appear homogeneously distributed in the matrix for each particle concentration without notable preferential orientation (see Fig. 2 and ESI).

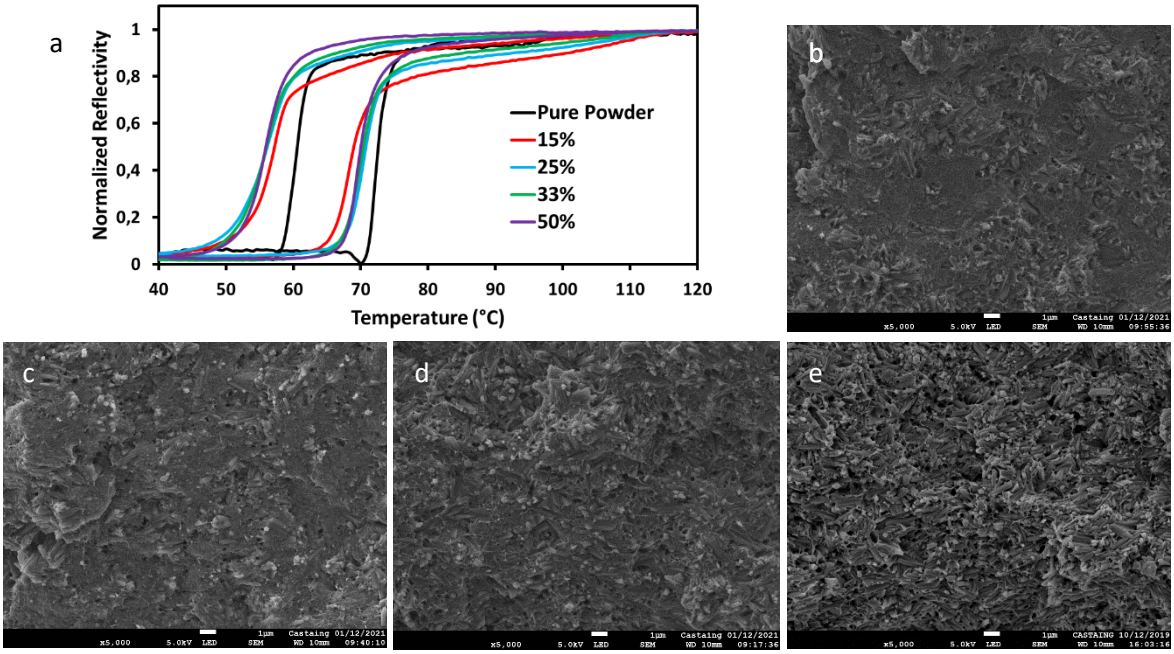

Fig. 2. SCO composites. a) Variable temperature optical reflectivity acquired simultaneously for the bulk powder of $[Fe(NH_2trz)_3]SO_4$ and for the $[Fe(NH_2trz)_3]SO_4$@P(VDF-TrFE) composites with different particle concentrations. (Note that the abrupt change of reflectivity refers to the SCO phenomeon, whereas the more gradual reflectivity changes at higher temperatures correspond to the Curie transition in the copolymer matrix - with increasing proportion for decreasing SCO load.). Selected SEM images of the SCO@polymer cross-sections for different particle concentrations b) 15%, c) 25%, d) 33% and e) 50%.

The open-loop free actuating behavior of the four actuators is shown in Figure 3a, which displays the cantilever tip displacement as a function of time in response to the highest current bias, which can be applied to the sample without damaging it, 1.3 A for sample **1**, 0.95 A for sample **2**, 1.25 A for sample **3** and 1.1 A for sample **4** (see Fig. S2 for the detailed open loop measurements). The maximum actuation amplitude of **1** is 4 mm and of **2** is 5.5 mm. It is important to notice that we have reproduced the preparation of sample **2** (sample **2'**), which presents very similar behavior with a maximum actuation amplitude of 5 mm (see Fig. S2), albeit for somewhat different applied bias (1.05 A) due to the slightly different resistivity of the silver layer. As it might be expected, the actuation range of **3** is significantly higher (8 mm), which represent a ca. 50 and 100 % increase with respect to **2** and **1**. This increment is roughly proportional to the increase of the SCO filler weight fraction. On the other hand, the actuation

range of **4** is somewhat lower than that of **3** despite the increase of the SCO concentration to 50 %. This finding denotes that there is a threshold concentration after which adding more active material does not lead to the increase of the actuation range. Most likely, for such high concentrations the homogeneity of the composite becomes compromised and particle-particle interactions tend to gain increasing role in the mechanical behavior of the composite (see SEM images in ESI). In open loop conditions, the steady-state position is reached in ca. 30-60 s for each actuator. Interestingly, one can notice a downward motion for actuators **3** and **4** at the start of the movement, which contributes to the increase of the response time. In the case of actuator **4,** this reverse motion is very important, with the actuator moving ca. 0.8 mm in the opposite direction before starting the actuation in the proper direction (see Fig. 3a). This downward motion seems to be caused by the intrinsic modification of the mechanical properties of the composite amplified by the increasing SCO concentration. At this point, it is worth to underline that a quantitative link between the SCO behaviour (Fig. 2a) and the actuating response (Fig. 3) is difficult to establish. Indeed, the spin transition in such Joule-heated bending actuators is intrinsically heterogeneous due to the inhomogeneous temperature distribution – as illustrated by the thermal mapping of the SCO layer of the actuator **2'** upon increasing current bias (Fig. S3), obtained with an IR camera.

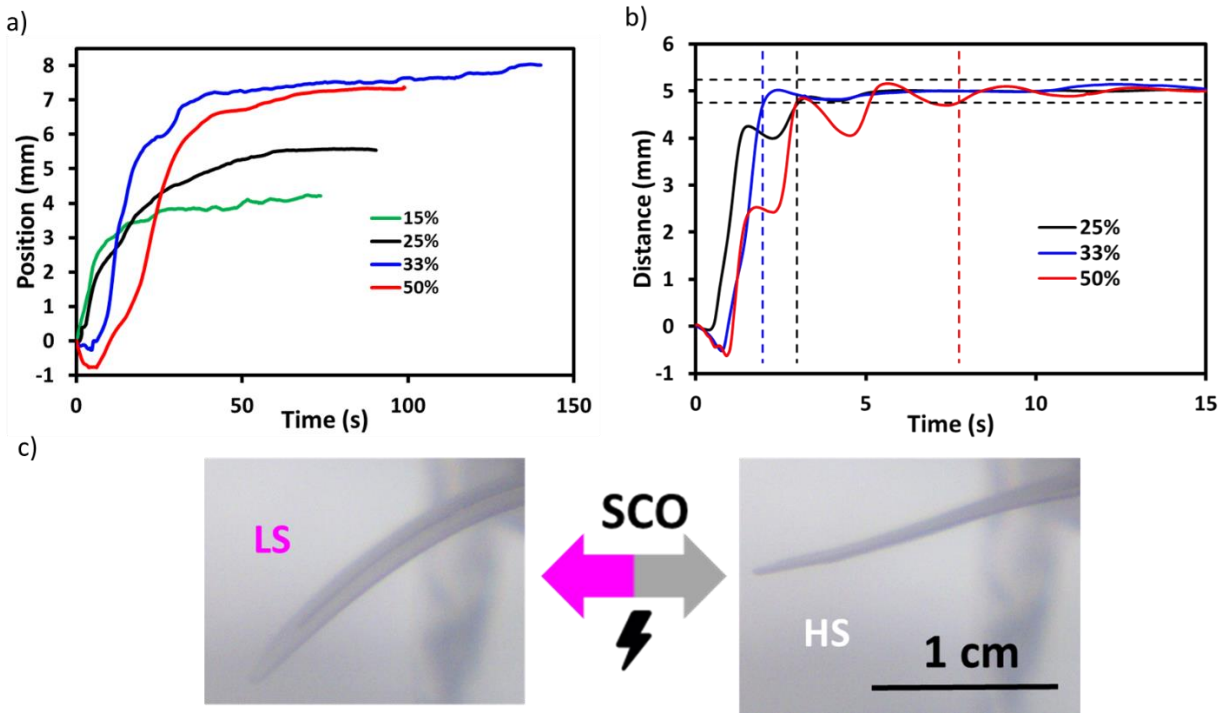

Fig. 3. Open- and closed-loop actuation behavior. a) Highest amplitude open-loop and b) fixed (5 mm) amplitude closed-loop actuation of the $[Fe(NH_2trz)_3]SO_4$ bilayer actuators fabricated

with different SCO filler concentrations. Horizontal dotted lines indicate the 5% error range and vertical dotted lines indicate the response time of the actuators. c) Photographs of a bilayer device (25 wt%) showing the bending movement between the LS and HS states.

To further analyse the concentration effect, actuators **2**, **3** and **4** were actuated in closed-loop conditions (without payload) to perform a fixed 5 mm displacement (Fig. 3b). The PID parameters were hand-tuned to reach an optimum value. Note that the maximum displacement of actuator **1** is only 4 mm, so the closed-loop behaviour of the latter is shown in a separate figure (Fig. S4). As it has been already shown in our previous work [22], a remarkable, ca. 1 order of magnitude improvement of the response time is obtained upon closed-loop control (vs. the open-loop values). (We define the response time as the time it takes for the actuator to reach the 5% error range of a given target position and remain stable inside this range). Notably, the closed-loop response time of actuators **1**-**3** falls in the range between 1.5 - 3 s. On the other hand, a significant slowdown of the closed-loop response is observed for actuator **4**, which is associated with a highly oscillatory response, compromising thus the controllability of the system.

Closed loop actuation of the samples while bearing a payload of 204 mg (approx. 3 times the actuator mass) is shown in Figures 4a-4b. The fixed displacement experiments with payloads (Fig. 4a and Fig. S4) reveal a significant "load robustness" in that the response of the actuators with payloads is comparable to their free actuation behavior discussed above. However, actuator **4**, having a higher energetic inertia due to the higher proportion of the SCO material, shows a highly oscillatory response, denoting a significant loss of controllability. However, while comparing the reverse motion with and without payload for the different actuators, a significant increase (from 0.8 to 2 mm) is only observed for actuator **4** and seems to result from the concomitant effect of the reduce stiffness of the composite and its own weight. It is interesting to notice also that, unlike for the free actuation, the response time of actuator **3** (4.25 s) is somewhat higher than that of actuator **2** (3.45 s), but such small differences lie within the experimental uncertainty. In order to further test the controllability of these devices, the actuators were then operated with the payloads using a sinusoidal position input under closed-loop conditions. Figure 4c and 4d shows these experiments for actuators **2** and **4**, respectively. In each case, the movement closely mirrors the given input, with a positioning error, which remains generally below 5 %. It is clear that the two systems retain high controllability once the initial energetic barrier has been cleared, showing that the difference

in controllability and performance between the actuators fabricated at different concentrations mostly pertains their actuation range and their behavior during the initial period of the actuation.

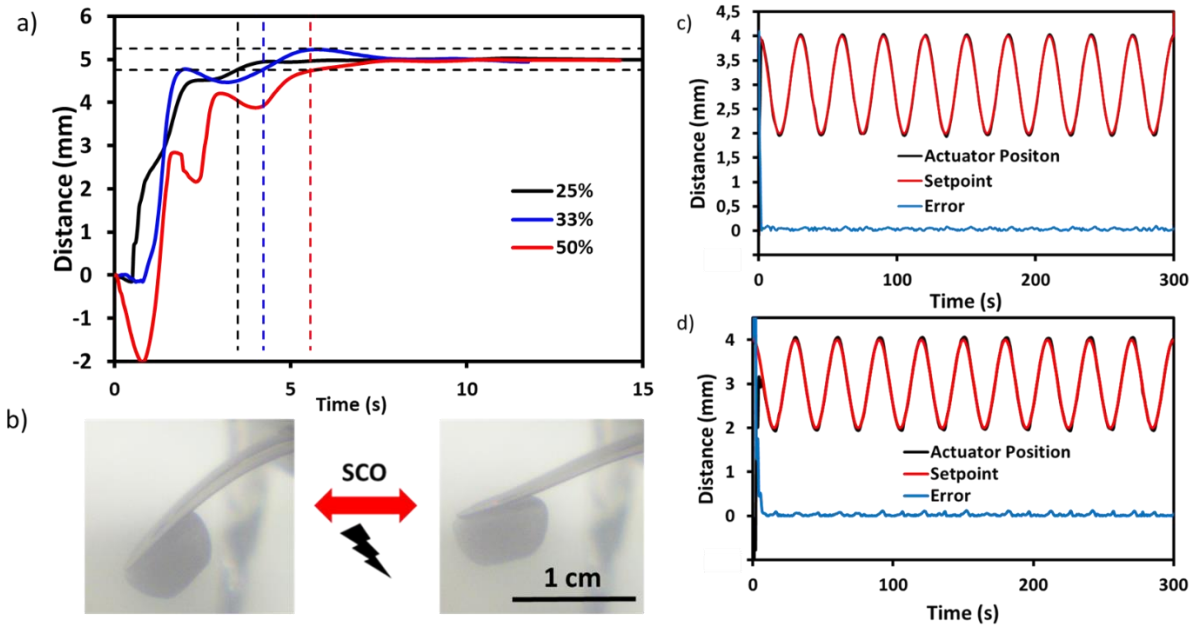

Fig. 4. Closed-loop actuation with payloads. a) Closed-loop step-wise actuation (target position = 5 mm) of the $[Fe(NH_2trz)_3]SO_4$ bilayer actuators with payload for different SCO filler concentrations (25, 33 and 50 %). Horizontal dotted lines indicate the 5% error range and vertical dotted lines indicate the response time of the actuators. b) Photographs of a bilayer device (25 wt%) with a payload of 204 mg showing the bending movement between the LS and HS states. (c-d) Closed-loop sinusoidal actuation of the actuators with payload for (c) 25 wt% and (d) 50 wt% of SCO filler concentration.

4. Conclusions

In summary, we fabricated and characterized electro-thermally actuated, bending bilayer $[Fe(NH_2trz)_3]SO_4$@P(VDF-TrFE)/Ag@P(VDF-TrFE) actuators with varying spin crossover filler concentrations. We have shown that the achievable actuating amplitude increases from ca. 4 to 8 mm when increasing the SCO filler fraction from 15 to 33 %, while keeping similar response times (ca. 30-60 s in open-loop and 2-3 s in closed-loop) and similar load-bearing capacity. On the other hand, a further increase of the SCO content to 50 % does not afford for higher amplitude movements and leads to reduced response times, which we attributed to the combined effects of the increased energetic barrier (for actuation) and reduced sample homogeneity. We expect that other SCO@polymer composite actuators will show a similar tendency for an optimum concentration, whose value must be determined case-by-case.

Indeed, the actuation performance is determined by a complex interplay between several parameters, such as the particle morphology, the device geometry, elastic and thermal properties of the materials and so forth, which must be optimized conjointly.

Funding This work received financial support from the Federal University of Toulouse/ Région Occitanie (PhD grant of MPB) and from the Agence Nationale de la Recherche (ANR-19-CE09-0008-01).

References

[1] M.D. Manrique-Juárez, S. Rat, L. Salmon, G. Molnár, C.M. Quintero, L. Nicu, H.J. Shepherd, A. Bousseksou, Coord. Chem. Rev. 308 (2016) 395–408.

[2] G. Molnár, S. Rat, L. Salmon, W. Nicolazzi, A. Bousseksou, Adv. Mater. 30 (2018) 1703862.

[3] H.J. Shepherd, I.A. Gural'Skiy, C.M. Quintero, S. Tricard, L. Salmon, G. Molnár, A. Bousseksou, Nat. Commun. 4 (2013) 1–9.

[4] P. Gütlich, A. Hauser, H. Spiering, Angew. Chemie Int. Ed. English. 33 (1994) 2024–2054.

[5] M.A. Halcrow, Chem. Soc. Rev. 40 (2011) 4119.

[6] P. Guionneau, Dalton. Trans. 43 (2014) 382–393.

[7] E. Collet, P. Guionneau, C. R. Chimie. 21 (2018) 1133–1151.

[8] P. Gütlich, H.A. Goodwin, eds., Spin Crossover in Transition Metal Compounds I, 1st ed., Springer Berlin Heidelberg, Berlin, Heidelberg (2004).

[9] M.A. Halcrow, Spin-Crossover Materials: Properties and Applications, Spin-Crossover Wiley (2013).

[10] I.A. Gural'Skiy, C.M. Quintero, J.S. Costa, P. Demont, G. Molnár, L. Salmon, H.J. Shepherd, A. Bousseksou, J. Mater. Chem. C. 2 (2014) 2949–2955.

[11] Y.C. Chen, Y. Meng, Z.P. Ni, M.L. Tong, J. Mater. Chem. C. 3 (2015) 945–949.

[12] Y.-S. Koo, J.R. Galán-Mascarós, Adv. Mater. 26 (2014) 6785–6789.

[13] S. Rat, M. Piedrahita-Bello, L. Salmon, G. Molnár, P. Demont, A. Bousseksou, Adv.

Mater. 30 (2018) 1705275.

[14] M. Piedrahita-Bello, L. Salmon, G. Molnar, P. Demont, B. Martin, A. Bousseksou, J. Mater. Chem. C., 8 (2020) 6042.

[15] R. Torres-Cavanillas, M. Morant-Giner, G. Escorcia-Ariza, J. Dugay, J. Canet-Ferrer, S. Tatay, S. Cardona-Serra, M. Giménez-Marqués, M. Galbiati, A. Forment-Aliaga, E. Coronado, Nat. Chem. 13 (2021) 1101–1109.

[16] M.D. Manrique-Juárez, F. Mathieu, A. Laborde, S. Rat, V. Shalabaeva, P. Demont, O. Thomas, L. Salmon, T. Leichle, L. Nicu, G. Molnár, A. Bousseksou, Adv. Funct. Mater. 28 (2018) 1801970.

[17] M.D. Manrique-Juarez, S. Rat, F. Mathieu, D. Saya, I. Séguy, T. Leïchlé, L. Nicu, L. Salmon, G. Molnár, A. Bousseksou, Appl. Phys. Lett. 109 (2016) 061903.

[18] M.D. Manrique-Juarez, F. Mathieu, V. Shalabaeva, J. Cacheux, S. Rat, L. Nicu, T. Leïchlé, L. Salmon, G. Molnár, A. Bousseksou, Angew. Chemie Int. Ed. 56 (2017) 8074–8078.

[19] J. Dugay, M. Giménez-Marqués, W.J. Venstra, R. Torres-Cavanillas, U.N. Sheombarsing, N. Manca, E. Coronado, H.S.J. van der Zant, J. Phys. Chem. C. 123 (2019) 6778–6786.

[20] M. Urdampilleta, C. Ayela, P.-H. Ducrot, D. Rosario-Amorin, A. Mondal, M. Rouzières, P. Dechambenoit, C. Mathonière, F. Mathieu, I. Dufour, R. Clérac, Sci. Rep. 8 (2018) 8016.

[21] M. Piedrahita-Bello, J.E. Angulo-Cervera, R. Courson, G. Molnár, L. Malaquin, C. Thibault, B. Tondu, L. Salmon, A. Bousseksou, J. Mater. Chem. C. 8 (2020) 6001–6005.

[22] M. Piedrahita-Bello, J.E. Angulo-Cervera, A. Enriquez-Cabrera, G. Molnár, B. Tondu, L. Salmon, A. Bousseksou, Mater. Horiz., 8 (2021) 3055–3062.

[23] L. G. Lavrenova, O. G. Shakirova, V. N. Ikorskii, V. A. Varnek, L. A. Sheludyakova, S. V. Larionov, Russ. J. Coord. Chem., 29, 1 (2003) 22–27.

[24] V. Y. Sirenko, O. I. Kucheriv, A. Rotaru, I. O. Fritsky,I. A. Gural'skiy, Eur. J. Inorg. Chem., (2020) 4523–4531.

[25] A. Grosjean, N. Daro, B. Kauffmann, A. Kaiba, J.-F. Létard, P. Guionneau, Chem. Commun., 47 (2011) 12382–12384.

[26] O. Roubeau, Chem. Eur. J., 18 (2012) 15230–15244

[27] L. Salmon, L. Catala, C. R. Chimie, 21 (2018) 1230–1269.

[28] A.M. Bazinenkov, D.A. Ivanova, A.P. Rotar', V.P. Mikhailov, IOP Conf. Ser. Mater. Sci. Eng. 781 (2020) 012007.

[29] V.R. Jayaneththi, K.C. Aw, A.J. McDaid, IEEE Int. Conf. Adv. Intell. Mechatronics (2017) 791–796.

[30] S. V. Ahir, A.M. Squires, A.R. Tajbakhsh, E.M. Terentjev, Phys. Rev. B. 73 (2006) 085420.

[31] A. Enriquez-Cabrera, A. Rapakousiou, M. Piedrahita Bello, G. Molnár, L. Salmon, A. Bousseksou, Coord. Chem. Rev., 419 (2020) 213396.